

A Robust Quantum Watermark Algorithm Based on Quantum Log-Polar Images

Zhiguo Qu¹(✉), Zhenwen Cheng², and Mingming Wang³

¹ Jiangsu Engineering Center of Network Monitoring,
Nanjing University of Information Science and Technology, Nanjing 210044,
People's Republic of China
qzghhh@126.com

² School of Electronic & Information Engineering,
Nanjing University of Information Science and Technology, Nanjing 210044,
People's Republic of China
czw381576996@163.com

³ School of Computer Science, Xi'an Polytechnic University, Xi'an 710048,
People's Republic of China
bluess1982@126.com

Abstract. Copyright protection for quantum image is an important research branch of quantum information technology. In this paper, based on quantum log-polar image (QUALPI), a new quantum watermark algorithm is proposed to better protect copyright of quantum image. In order to realize quantum watermark embedding, the least significant qubit (LSQb) of quantum carrier image is replaced by quantum watermark image. Compared to previous quantum watermark algorithms, the new algorithm effectively utilizes two important properties of log-polar sampling, i.e., rotation and scale invariances. These invariances make quantum watermark image extracted have a good robustness when stego image was subjected to various geometric attacks, such as rotation and scaling. Experimental simulation based on MATLAB shows that the new algorithm has a good performance on robustness, transparency and capacity.

Keywords: Quantum watermark algorithm · Quantum log-polar image · Least significant qubit · Robustness

1 Introduction

With the rapid development of quantum communication network, in order to achieve safe and efficient transmission of quantum image information in quantum communication network, people began to study using quantum states to store and transfer digital image information in the decades. Moreover, with widespread applications of quantum image in quantum communication network, quantum watermark also has emerged to protect copyright of quantum image, which is fulfilled by embedding watermark image consisting of the information related to copyright owner into carrier image. So far, quantum image representation methods and quantum watermark algorithms have made a lot of achievements.

At present, the major achievements of quantum image representation methods, i.e., Qubit Lattice [1], Entangled Image [2], Real Ket [3], flexible representation of quantum images (FRQI) [4], novel enhanced quantum representation (NEQR) [5], quantum log-polar image (QUALPI) [6] and novel quantum representation of color digital images (NCQI) [7], have been proposed. Among of them, quantum images of QUALPI representation can easily perform some complex geometric transformations, such as rotation and scaling. With the increasing importance of images in people's daily life, color image analysis by quaternion Zernike moments (QZMs) [8], content-based image retrieval (CBIR) [9] and digital image forensics [10] also have been widely studied.

In the aspect of quantum watermark algorithms, analysis and improvement of the watermark strategy for quantum images based on quantum Fourier transform [11] was proposed by Yang et al. In 2013 and 2014, Song et al. put forward two dynamic watermarking schemes for quantum image based on quantum wavelet transform [12] and Hadamard transform [13], respectively. This two quantum watermark algorithms have a larger capacity and good transparency. The least significant bit (LSB [14]) modification is one of the most important methods in classical digital watermark, which has advantages of easy operation and large amount of information hiding. In 2016, a least significant qubit (LSQb) algorithm for quantum image based on NCQI representation [15] was proposed by Sang.

From the achievements given above, it can be found out that the current quantum watermark technology is still on the early stage of its development. Most of algorithms have not yet begun to discuss the robustness of watermark image, especially on geometric attacks. In view of widespread applications and universality of geometric distortion attacks in quantum image processing, most of watermarked quantum images are invulnerable to resist this kind of attacks. In order to make up for the drawbacks of existing quantum watermark algorithms, this paper proposes a novel robust quantum watermark algorithm based on the QUALPI representation. By combining the QUALPI representation model with the LSQb modification technique, the new algorithm enables to effectively resist geometric distortions or attacks, so as to better protect copyright of quantum image.

The rest of the paper is organized as follows. Section 2 introduces the preliminary knowledge related to the new algorithm. In Sect. 3, the novel robust quantum watermark algorithm is described in detail. The simulation results and performance analysis are given in Sect. 4. Finally, a conclusion and the future work are provided in Sect. 5.

2 Preliminaries

2.1 The QUALPI Image Representation and Rotation Transformation

In QUALPI, the sampling resolutions of the log-radius and the angular orientations of a log-polar image are assumed to be 2^m and 2^n respectively. For this image, the quantum image representation can be expressed as shown in the following equation:

$$|I\rangle = \frac{1}{\sqrt{2^{m+n}}} \sum_{\rho=0}^{2^m-1} \sum_{\theta=0}^{2^n-1} (|g(\rho, \theta)\rangle \otimes |\rho\rangle \otimes |\theta\rangle) \tag{1}$$

The position information of a pixel is represented by (ρ, θ) , where ρ denotes the log-radius and θ represents the angular position. The gray scale of the corresponding pixel is represented by $g(\rho, \theta)$. The gray range of this image is assumed to be 2^q . Thus the gray scale can be encoded by binary sequence $C_{q-1}C_{q-2} \cdots C_1C_0$ as follow:

$$g(\rho, \theta) = C_{q-1}C_{q-2} \cdots C_1C_0, g(\rho, \theta) \in [0, 2^{q-1}] \tag{2}$$

Reference [6] discusses the quantum arbitrary rotation transformation of the QUALPI quantum image model. Assume that a rotation transformation R_x for quantum image will be operated and the rotation angle can be encoded by binary sequence $r_{n-1}r_{n-2} \cdots r_1r_0$ as follow:

$$R_x = r_{n-1}r_{n-2} \cdots r_1r_0, r_i \in \{0, 1\}, R_x \in [0, 2^n - 1] \tag{3}$$

Thus, when R_x rotation is performed, the procedure can be divided into n sub-operations. If $r_i = 0$, none operation will be done for the i th sub-operation. Otherwise, a 2^i rotation R_{2^i} will be performed on quantum image.

The quantum 2^k rotation U_{2^k} will add the angular positions of every pixel by $2^k \pmod{2^n}$. Specifically, this operation aims to make a unit shift for the highest $(n - q)$ qubits of the angular sequence $|\theta\rangle$ in the QUALPI quantum image.

2.2 Quantum Bit Comparator

In order to embed watermark image into carrier image by using LSQb modification, it is necessary to compare the state of the last qubit of a pixel in the same position of those two images by using quantum bit comparator. According to the results of the comparator, the corresponding unitary operation is performed on carrier image. Consequently, this section describes a specific quantum bit comparator.

In 2012, Wang et al. gave a quantum comparator to judge whether two qubits are same or not in Ref. [16]. As shown in Fig. 1, $|a\rangle, |b\rangle$ are the input qubits and $|c\rangle, |d\rangle$ denote the outputs of the corresponding states.

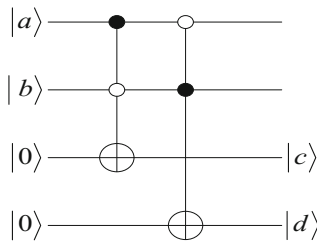


Fig. 1. Two qubit comparator.

If $|c\rangle|d\rangle = |1\rangle|0\rangle$ or $|c\rangle|d\rangle = |0\rangle|1\rangle$, then quantum state $|a\rangle$ is not equal to quantum state $|b\rangle$. If $|c\rangle|d\rangle = |0\rangle|0\rangle$, then quantum state $|a\rangle$ is equal to quantum state $|b\rangle$.

3 A Robust Quantum Watermark Algorithm

In this section, the main steps of new algorithm including embedding watermark process and extracting watermark process are presented in details. The embedding process is mainly based on the QUALPI representation and the LSQb modification technique, and the extracting process is the inverse of the embedding process.

3.1 Embedding Watermark Process

The flow chart of the embedding process is shown in Fig. 2 and steps of the embedding process are given as follows:

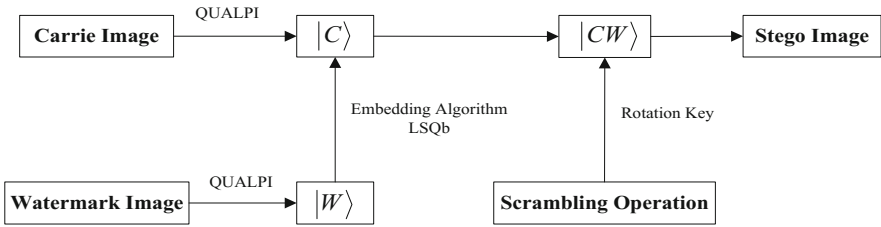


Fig. 2. The flow chart of embedding watermark process.

Step (1): In this paper, the size of carrier image is equal to the size of watermark image. The QUALPI expressions of carrier image and watermark image are shown in Eqs. (4) and (5), respectively:

$$|C\rangle = \frac{1}{\sqrt{2^{m+n}}} \sum_{\rho=0}^{2^m-1} \sum_{\theta=0}^{2^n-1} |c_{q-1}c_{q-2} \cdots c_1c_0\rangle |\rho\theta\rangle \tag{4}$$

$$|W\rangle = \frac{1}{\sqrt{2^{m+n}}} \sum_{\rho=0}^{2^m-1} \sum_{\theta=0}^{2^n-1} |w_0\rangle |\rho\theta\rangle \tag{5}$$

where $|c_{0_j}\rangle$ and $|w_{0_j}\rangle$ denotes the state of the last qubit of the (ρ_j, θ_i) pixel in carrier image and watermark image, respectively, which are used as inputs into the quantum comparator. According to the results of the comparator, the corresponding unitary operation is performed on carrier image to complete the LSQb modification.

Step (2): If the outputs from the quantum comparator are equal, then it will do nothing about carrier image. In this case, the following unitary transformation will be performed.

$$U_{s_{ji}} = I^{\otimes q} \otimes \left(\sum_{\rho=0}^{2^m-1} \sum_{\theta=0}^{2^n-1} |\rho\theta\rangle\langle\rho\theta| \right) \tag{6}$$

Step (3): However, if the outputs are different, the following unitary transformation will be performed on the state of quantum carrier image.

$$U_{D_{ji}} = I^{\otimes q-1} \otimes U \otimes |ji\rangle\langle ji| + I^{\otimes q} \otimes \left(\sum_{\rho=0}^{2^m-1} \sum_{\theta=0, \rho\theta \neq ji}^{2^n-1} |\rho\theta\rangle\langle\rho\theta| \right) \tag{7}$$

where

$$U = \sigma_X = \begin{bmatrix} 0 & 1 \\ 1 & 0 \end{bmatrix} \tag{8}$$

It is obvious that the unitary U is the CNOT gate. Next, the concrete derivation process is given.

$$\begin{aligned} U_{D_{ji}}(|C\rangle) &= \left(I^{\otimes q-1} \otimes U \otimes |ji\rangle\langle ji| + I^{\otimes q} \otimes \sum_{\rho=0}^{2^m-1} \sum_{\theta=0, \rho\theta \neq ji}^{2^n-1} |\rho\theta\rangle\langle\rho\theta| \right) \\ &\quad \left(\frac{1}{\sqrt{2^{m+n}}} \sum_{\rho=0}^{2^m-1} \sum_{\theta=0}^{2^n-1} |c_{q-1}c_{q-2} \cdots c_1c_0\rangle |\rho\theta\rangle \right) \\ &= \frac{1}{\sqrt{2^{m+n}}} \left(I^{\otimes q-1} \otimes U \otimes |ji\rangle\langle ji| + I^{\otimes q} \otimes \sum_{\rho=0}^{2^m-1} \sum_{\theta=0, \rho\theta \neq ji}^{2^n-1} |\rho\theta\rangle\langle\rho\theta| \right) \\ &\quad \left(|c_{q-1}^j c_{q-2}^j \cdots c_1^j c_0^j\rangle |ji\rangle + \sum_{\rho=0}^{2^m-1} \sum_{\theta=0, \rho\theta \neq ji}^{2^n-1} |c_{q-1}c_{q-2} \cdots c_1c_0\rangle |\rho\theta\rangle \right) \\ &= \frac{1}{\sqrt{2^{m+n}}} \left(|c_{q-1}^j c_{q-2}^j \cdots c_1^j c_0^j\rangle |ji\rangle + \right. \\ &\quad \left. \sum_{\rho=0}^{2^m-1} \sum_{\theta=0, \rho\theta \neq ji}^{2^n-1} |c_{q-1}c_{q-2} \cdots c_1c_0\rangle |\rho\theta\rangle \right) \end{aligned} \tag{9}$$

where

$$|\bar{c}_0^{ji}\rangle = \begin{cases} |0\rangle, |c_0^j\rangle = 1 \\ |1\rangle, |c_0^j\rangle = 0 \end{cases} \tag{10}$$

Step (4): By repeating the three steps above, watermark image is embedded into carrier image by the LSBq modification. Finally, as it is described in Sect. 2.1, stego image will be made a rotation transformation R_x . The rotation angle can be determined according to the key, named as K_1 , shared by two parties of communication in advance.

3.2 Extracting Watermark Process

The flow chart of the extracting process is shown in Fig. 3. Its main steps can be described as follows.

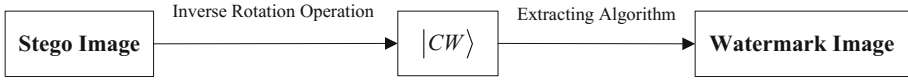


Fig. 3. The flow chart of extracting watermark process.

Step (1): According to the K_1 , two parties of communication will share an another key, named as K_2 , in order to restore the original stego image. Another rotation transformation can be performed on stego image.

Step (2): It is clear that the LSQB of stego image is a complex vector in Hilbert space which the size is 2^{q+m+n} . So let decompose the vector into the direct product of color and correspondingly position firstly. Taking a $2^1 \times 2^2$ log-polar image with gray rang 2^q as an example, the stego image vector is Q . Then the disintegrated vector Q is given as the following form:

$$Q = a_0 \otimes \begin{pmatrix} 1 \\ 0 \\ 0 \\ \vdots \\ 0 \\ 0 \end{pmatrix} + a_1 \otimes \begin{pmatrix} 0 \\ 1 \\ 0 \\ \vdots \\ 0 \\ 0 \end{pmatrix} + \cdots + a_6 \otimes \begin{pmatrix} 0 \\ 0 \\ 0 \\ \vdots \\ 1 \\ 0 \end{pmatrix} + a_7 \otimes \begin{pmatrix} 0 \\ 0 \\ 0 \\ \vdots \\ 0 \\ 1 \end{pmatrix} \quad (11)$$

Obviously, this step can be realized because the vector Q and the binary encoding of position are known. After converting every first part (color information) of the direct product to binary data, the number of binary bit is equivalent to the number of bits of the stego image's color encoding. In this example, it means converting $a_0, a_1, \dots, a_6, a_7$ to the appropriate binary data $a_{0_b}, a_{1_b}, \dots, a_{6_b}, a_{7_b}$. The a_{i_b} stands for the gray's binary sequence of the i th pixel in stego image.

Step (3): The last step is to extract the last bit of every binary data. According to the preparation of QUALPI state in Ref. [6], these bits information is restored to the original watermark image.

In general, the extracting process of watermark image is an inverse process of embedding watermark.

4 The Experiment Result and Performance Analysis

This section gives some simulation-based experiments and analysis of the results and performance of the proposed quantum watermark algorithm. All experiments are simulated on the MATLAB R2012a.

There are three factors of performance evaluation for quantum watermark algorithms, including robustness, transparency and capacity, respectively. Robustness shows that watermark image can be extracted effectively from stego image after various attacks. Transparency represents the similarity between carrier image and stego image. Capacity is the maximum amount of watermark information embedded into carrier image without affecting its normal use. It can be represented by the number of bits of watermark information contained in the unit carrier image pixel. Three images “Baboon”, “Cameraman” and “Lena” are used in the experiments as carrier images. Four images “Eagle”, “Recycling”, “Thumbs-up” and “HTC” are used as watermark images. The image sizes for carrier and watermark are all $2^7 \times 2^8$.

4.1 Robustness

In defending various geometric attacks, the new algorithm effectively utilizes two important properties of log-polar sampling, i.e., rotation and scale invariances. These invariances make quantum watermark image extracted have a good robustness when stego image was subjected to various geometric attacks, such as rotation, vertical axisymmetry, horizontal axisymmetry and scaling.

In order to prove the above argument, Figs. 4, 5, 6 and 7 are given respectively to represent above-mentioned geometric attacks. The experimental results show that watermark image can be extracted effectively after a variety of attacks, and has a high image quality. It means that the new algorithm has good robustness.



Fig. 4. Rotation attack. (a) The stego image attacked by rotation, (b) the stego image restored by the quantum image registration algorithm, (c) the watermark image extracted from (b).



Fig. 5. Vertical axisymmetry. (a) The stego image attacked by horizontal axisymmetry, (b) the stego image restored, (c) the watermark image extracted from (b).



Fig. 6. Horizontal axisymmetry. (a) The stego image attacked by vertical axisymmetry, (b) the stego image restored, (c) the watermark image extracted from (b).



Fig. 7. Scaling attack. (a) The stego image attacked by scaling, (b) the stego image restored, (c) the watermark image extracted from (b).

4.2 Transparency

At present, there is no specific evaluation standard for visual quality index of the quantum image. Therefore, in this paper, the classical PSNR (Peak Signal-to-Noise Ratio) is applied to evaluate transparency of the quantum watermark.

Assuming there are two $2^m \times 2^n$ images I and J with gray range 2^q (I is the original carrier image, J is the embedded carrier image). $I(\rho, \theta)$ and $J(\rho, \theta)$ represents the pixel values of the (ρ, θ) pixel. MSE (Mean Squared Error) and PSNR are defined as Eqs. (12) and (13), respectively:

$$MSE = \frac{1}{mn} \sum_{\rho=0}^{2^m-1} \sum_{\theta=0}^{2^n-1} [I(\rho, \theta) - J(\rho, \theta)]^2 \quad (12)$$

$$PSNR = 20 \times \log_{10} \left(\frac{MAX_I}{\sqrt{MSE}} \right) \quad (13)$$

Here, MAX_I is the maximum possible pixel value of the image.

From the experimental results in Fig. 8, it is easy to know that stego image and the original carrier image are incapable to be identified by the naked eye of human being.

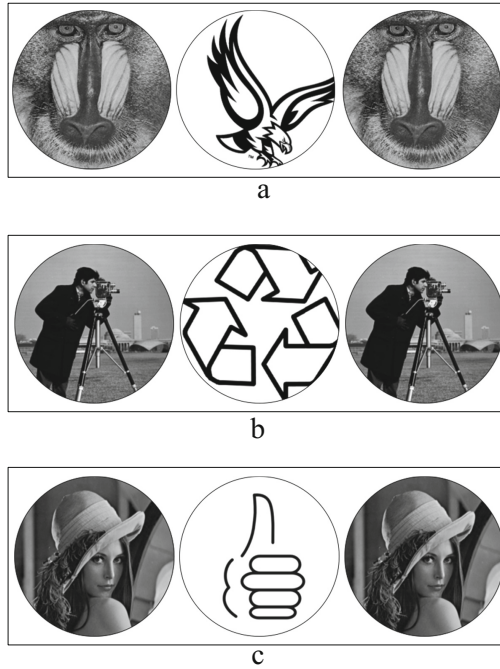


Fig. 8. In three groups of pictures, the left are the original carrier images, the middle are the watermark images, the right are the embedded carrier images.

Table 1 lists out the PSNR values of stego image obtained by embedding different watermark images into the same carrier image, respectively. And Fig. 9 shows the change of PSNR values of Table 1. It can be found that the PSNR values of stego images are much higher than the image quality standard of 38 dB, which proves they have high image qualities. Therefore, the new algorithm can obtain good transparency.

Table 1. PSNR values of stego images in our simulation.

PSNR(dB) Carrier image	Watermark image	Eagle	Recycling	Thumbs-up	HTC
	Baboon		46.1551	46.1515	46.1482
Cameraman		46.1133	46.0789	46.0832	46.1029
Lena		46.1051	46.1064	46.1074	46.0977

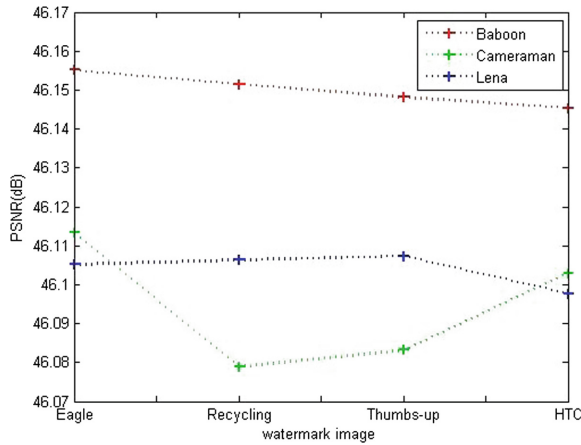


Fig. 9. The change of PSNR values of Table 1.

4.3 Capacity

Capacity can be accurately calculated by the embedding rate, which is denoted by the number of bits embedded divided by all the least significant qubits of the carrier image in this paper. It is easy to know the embedding rate of the new algorithm is equal to 1. Furthermore, based on LSQb modification in our algorithm, the modifying rate of the algorithm is 0.5, which means that half of the qubits need to be modified, and the other half is not. Comparing with the previous achievements, the embedding rate and them modifying rate of our algorithm is rather good.

5 Conclusion

In this paper, a novel robust watermarking algorithm is proposed. By combining the QUALPI representation model with the LSQb modification technique, new algorithm enables to effectively resist geometric distortion or rotation attacks, so as to better protect the copyright of quantum image. The simulation results based on MATLAB show that the new algorithm has a good performance in robustness and transparency. On the basis of the capacity analysis to the new algorithm, the embedding rate of our algorithm is 1 and the modification rate is 0.5.

The robustness of the quantum watermark image against geometric attacks has been improved in this paper. But it does not discuss more complex attacks, such as geometric zooming and tailoring. Therefore, the next research will be focused on the design of quantum robust watermark algorithm to deal with these complex attacks in the future.

Acknowledgments. This work was supported by the National Natural Science Foundation of China (Nos. 61373131, 61303039, 61232016, 61501247), Sichuan Youth Science and Technique Foundation (No. 2017JQ0048), NUIST Research Foundation for Talented Scholars (2015r014), PAPD and CICAET funds.

References

1. Venegas-Andraca, S.E., Bose, S.: Storing, processing and retrieving an image using quantum mechanics. In: Proceedings of the SPIE Conference on Quantum Information and Computation, vol. 5105, pp. 1085–1090 (2003)
2. Venegas-Andraca, S.E., Ball, J.L., Burnett, K., Bose, S.: Processing images in entangled quantum systems. *Quantum Inf. Process.* **9**, 1–11 (2004)
3. Latorre, J.I.: Image compression and entanglement. *Computer Science* (2005)
4. Le, P.Q., Dong, F.Y., Hirota, K.: A flexible representation of quantum images for polynomial preparation, image compression, and processing operations. *Quantum Inf. Process.* **10**, 63–84 (2011)
5. Zhang, Y., Lu, K., Gao, Y.H.: NEQR: a novel enhanced quantum representation of digital images. *Quantum Inf. Process.* **12**, 2833–2860 (2013)
6. Zhang, Y., Lu, K., Gao, Y.H., Xu, K.: A novel quantum representation for log-polar images. *Quantum Inf. Process.* **12**, 3103–3126 (2013)
7. Sang, J.Z., Wang, S., Li, Q.: A novel quantum representation for color digital images. *Quantum Inf. Process.* **16**, 16–42 (2016)
8. Chen, B.J., Shu, H.Z., Coatrieux, G., Chen, G., Sun, X.M., Coatrieux, J.L.: Color image analysis by quaternion-type moments. *J. Math. Imaging Vis.* **51**, 124–144 (2015)
9. Xia, Z.H., Wang, X.H., Zhang, L.G., Qin, Z., Sun, X.M., Ren, K.: A privacy-preserving and copy-deterrence content-based image retrieval scheme in cloud computing. *IEEE Trans. Inf. Forensics Secur.* **11**, 2594–2608 (2016)
10. Wang, J.W., Li, T., Shi, Y.Q., Lian, S.G., Ye, J.Y.: Forensics feature analysis in quaternion wavelet domain for distinguishing photographic images and computer graphics. *Multimedia Tools Appl.* 1–17 (2016)
11. Yang, Y.G., Jia, X., Xu, P., Tian, J.: Analysis and improvement of the watermark strategy for quantum images based on quantum Fourier transform. *Quantum Inf. Process.* **12**, 793–803 (2013)
12. Song, X.H., Wang, S., Liu, S., El-Latif, A.A., Niu, X.M.: A dynamic watermarking scheme for quantum images using quantum wavelet transform. *Quantum Inf. Process.* **12**, 3689–3706 (2013)
13. Song, X.H., Wang, S., El-Latif, A.A., Niu, X.M.: Dynamic watermarking scheme for quantum images based on Hadamard transform. *Multimedia Syst.* **20**, 379–388 (2014)
14. Shailender, G., Bhushan, A.G.: Information hiding least significant bit steganography and cryptography. *Int. J. Mod. Educ. Comput. Sci.* **4**, 27–34 (2012)
15. Sang, J.Z., Wang, S., Li, Q.: Least significant qubit algorithm for quantum images. *Quantum Inf. Process.* **15**, 1–20 (2016)
16. Wang, D., Liu, Z.H., Zhu, W.N., Li, S.Z.: Design of quantum comparator based on extended general Toffoli gates with multiple targets. *Comput. Sci.* **39**, 302–306 (2012)